Thermo-mechanical behavior in precision motion control: Unified framework for fast and accurate FRF identification.

Enzo Evers
Department of Mechanical Engineering
Control Systems Technology
Eindhoven University of Technology
Email: E.Evers@tue.nl

Bram de Jager
Department of Mechanical Engineering
Control Systems Technology
Eindhoven University of Technology
Email: A.G.de.Jager@tue.nl

Tom Oomen
Department of Mechanical Engineering
Control Systems Technology
Eindhoven University of Technology
Email: T.A.E.Oomen@tue.nl

***Abstract*—The achievement of higher accuracy and throughput in mechatronic systems using motion control has led to the situation where the thermal effects in mechatronic systems have become increasingly important and have to be actively controlled. In view of achieving overall control performance of interacting thermal and mechanical dynamics, in this paper it is aimed to develop an identification approach that delivers the required model for thermo-mechanical control. A novel technique is developed that leads to a significant reduction in both the estimation error and measurement time compared to traditional identification methods. The proposed approach is applied to a thermo-mechanical system in an extensive experimental study.**

I. Introduction

Accuracy and throughput requirements on precision mechatronic systems are becoming ever more stringent. Keeping up with Moore's law requires an ever increasing accuracy of position control of waferscanners [1]. Also, enabling increasingly small feature detection in electron microscopy requires the use of advanced control methods for drift compensation [2].

These increasing requirements have spurred the development of advanced techniques [3] for the control of servo, i.e., electro-mechanical, systems. Moreover, overall performance of systems-of-systems is increasingly important, by exploiting inter-system coupling techniques [4], traditional performance limitations are partially mitigated. This has resulted in a large range of advanced control techniques that are readily applied to precision mechatronic systems, e.g., advanced inversion based feedforward [5], [6], multirate feedforward [7], and iterative learning control [8].

Thermal effects in mechatronic control systems have long been negligible in the overall system performance. However, in part due to advances in servo control, this is no longer the case. In fact, thermally induced deformations are at present a dominant source of drift in electron microscopy [2] and overlay error in waferscanning applications. Moreover, there has been significantly less research effort spent towards controlling thermal disturbances in mechatronic systems, and therefore the thermal modeling, identification, and control of thermal and thermo-mechanical systems is not yet fully exploited.

At present, thermal control is often limited to PID-like controllers, controlling the local temperature at a sensor location to a (constant) setpoint. While in general, the position accuracy at the point-of-interest (POI) is influenced by the full temperature distribution, i.e., thermal gradients induce internal stress and deformations due thermal expansion. Local control is often insufficient in achieving the required performance at the POI [9], since this does not guarantee the absence of thermal gradients over the full system. Therefore, inferential control techniques [10] are required that take into account the full temperature distribution as opposed to solely considering the local measurements. For instance, the inferential control problem [11] is approached using a model-based control design, since this would allow for the estimation of the global temperature field using local sensor measurements. By then assuming a static mapping between the temperature field and deformation, valid for a limited temperature range, this allows the estimation of the deformation at the POI. Furthermore, this facilitates the use of error-compensation techniques as illustrated in [12], [4].

Although active control of thermo-mechanical behavior is promising, a model of the spatial temperature distribution is essential. Constructing a model to reconstruct the deformation at the POI is non-trivial, see, e.g., [13], [14] for related work on servo systems. The main challenge lies in determining a model that predicts the thermo-mechanical deformation which can subsequently be used for compensation.

The main contribution of this paper is to provide the first step towards expanding the advanced servo identification and control techniques to encompass thermo-mechanical systems. This is done by approaching the problem from a black-box point of view, starting with system identification techniques to construct a non-parametric model of the thermal system response, e.g., Frequency Response Function (FRF) identification [15]. The key challenge lies in developing a FRF identification that is fast, inexpensive and accurate.

The non-parametric models can be used directly, e.g., in controller tuning [16], as a basis for stability analysis in coupled-systems [4], or as initial step in further parametric

978-1-5090-6684-1/18/$31.00

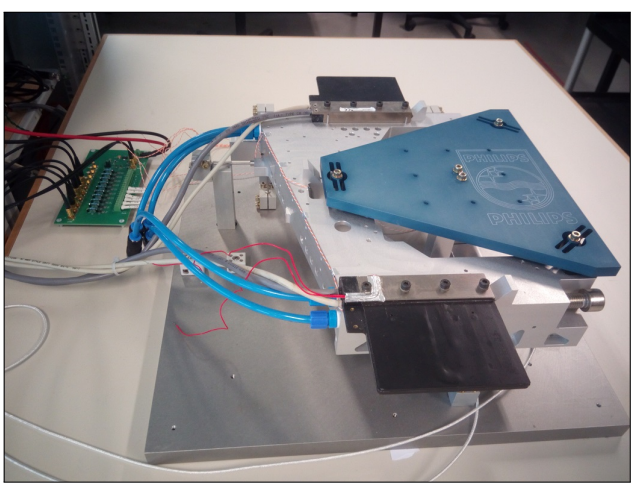

(a) Photograph

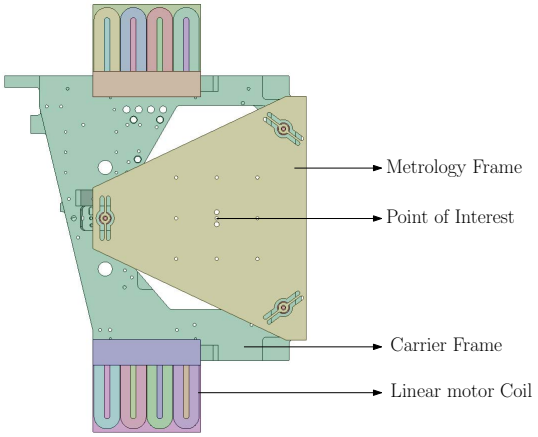

(b) CAD rendering

Fig. 1: Photograph and CAD rendering of the Precision Stage Application (PSA) setup, which is an typical industrial precision mechatronic system. It shows the carrier frame with linear motor coils and metrology frame. The carrier frame is connected to a baseplate in all 6 DOF's by flexure wires, serving as a metrology reference. The linear motor coils are used to generate heat, that induces stress and deformation in the carrier frame.

identification [17]. Examples include mechatronics and flexible dynamics in [18], [19], thermal systems in [9], [20] and electrical systems in [21] and combustion systems in [22].

The main contributions of this paper are:

- C1 A new approach to non-parametric FRF system identification using local parametric models.
- C2 An extensive experimental study where the proposed approach is applied to an industrial precision thermo-mechanical setup.

The outline of this paper is as follows: First, the identification procedure is developed based on a local parametric modeling approach building on the Local Rational Method with Prescribed poles (LRMP) approach as presented in [23]. The developed method is compared to classical identification procedures such as the spectral method [15] and key differences are highlighted. Second, the proposed approach is applied to the experimental system, shown in Fig. 1, in an extensive case study. And finally, conclusions based on results in the case study are presented.

II. System identification using local parametric models

In this section, a new FRF identification approach is presented and compared to classical spectral analysis [15], thereby constituting contribution C1.

Consider the response of a discrete Linear Time Invariant (LTI) system to an excitation input $u(n)$, see, e.g., an example in Fig. 2, then the output $y(n)$ can be written as

$$y(n) = \sum_{k=-\infty}^{\infty} u(k)g(n-k) + v(n) \tag{1}$$

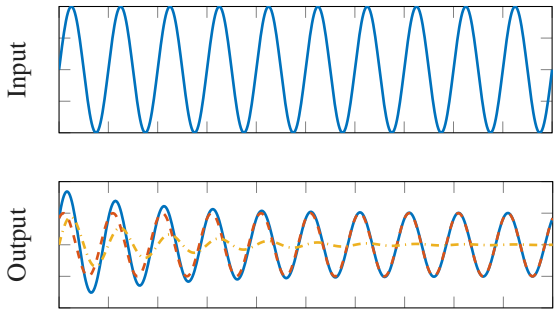

Fig. 2: Example of a system response (——), composed of a steady state response (- - -) and a transient component (-·-·-).

where $g(n)$ denotes the impulse response of the system and $v(n)$ the output noise corruption. By then applying a Discrete Fourier Transform (DFT)

$$X(k) = \frac{1}{\sqrt{N}} \sum_{n=0}^{N-1} x(n) e^{\frac{-i2\pi kn}{N}} \tag{2}$$

on a finite interval of (1) the convolution can be represented as a multiplication

$$Y(k) = G(e^{i\omega_k})U(k) + T(e^{i\omega_k}) + V(k) \tag{3}$$

in the Fourier domain, where $G(e^{i\omega_k})$ is the frequency response function of the dynamic system, $Y(k), U(k), V(k)$ are the DFT of $y(n), u(n), v(n)$ and k denotes the k-th frequency bin. Here, $T(e^{i\omega_k})$ accounts for the transients for both the system response $T_G(e^{i\omega_k})$ and the noise $T_V(e^{i\omega_k})$. The transient terms account for the initial condition of the

system, i.e., the transition of an infinite to a finite interval. By adding these transient terms, relation (3) is again an exact representation.

A. Spectral analysis method

In many mechatronic systems, the spectral analysis methods are still commonly used. These methods construct the non-parametric transfer function of the dynamical system by using estimates of the cross-power and auto-power spectra of the input and output signals.

Consider the relation in (1) then the FRF estimate of the system using spectral methods [15, Sec 7.2.3.] is

$$G(e^{i\omega_k}) = S_{yu}(e^{i\omega_k})S_{uu}^{-1}(e^{i\omega_k}) \tag{4}$$

where $S_{yu}(e^{i\omega_k}), S_{uu}(e^{i\omega_k})$ are the cross- and autopower spectra of the input-output signals. These are replaced by their estimates, constructed by dividing the input-output data into P (non-)overlapping segments. However, these segments are often not perfectly periodic, due to transients and noise, see (3), therefore often a window function is applied [15], e.g., a Hanning window. This results in

$$\hat{G}(e^{i\omega_k}) = \hat{S}_{Y_wU_w}(k)\hat{S}_{U_wU_w}^{-1}(k) \tag{5}$$

where $\hat{S}_{Y_wU_w}(k), \hat{S}_{U_wU_w}^{-1}(k)$ are the weighted estimated cross- and autopower spectrum, e.g.,

$$\hat{S}_{Y_wU_w}(k) = \frac{1}{P}\sum_{p=1}^{P} Y_w^{(p)}(k)(U_w^{(p)})^H \tag{6}$$

where the weighted, using window $w(t)$, DFT transformation is

$$Y_w^{(p)}(k) = \frac{1}{\sqrt{\sum_{t=0}^{N/P-1}|w(t)|^2}} \sum_{t=0}^{N/P-1} w(t)y(t+(p-1)N/P)e^{-j2\pi kt/N} \tag{7}$$

Using this method, the frequency response function $\hat{G}(e^{i\omega_k})$ is estimated from the input-output data. However, clearly, the estimate is influenced by transients induced by any non-periodic data, i.e., not periodic in N/P samples of the segment size. By applying the window function, prior knowledge is used to perform a bias/variance trade-off and reduce the transients effects on the FRF estimation $\hat{G}(e^{i\omega_k})$. By selecting a different window function, e.g. boxcar, diff or Hanning window, a different assumed smoothness can be imposed on the estimated function.

B. Local Rational Method with Prescribed poles (LRMP)

Consider again the relation in (3), here an estimation $T(e^{i\omega_k})$ is desired such that the estimate of $G(e^{i\omega_k})$ can be compensated for transient contributions. To construct this transient estimate, a local parametric modeling approach is used [23]. In this approach, it is assumed that both $G(e^{i\omega_k})$ and $T(e^{i\omega_k})$ are smooth, similarly assumed in the spectral analysis

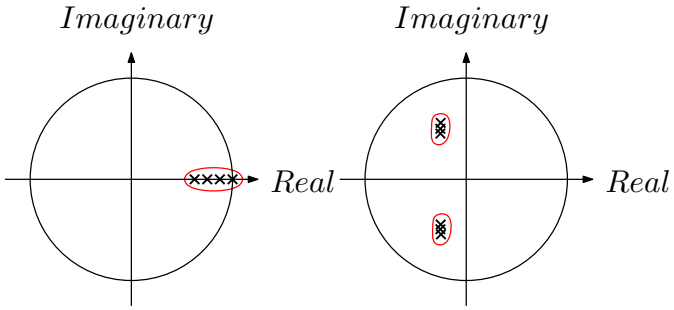

(a) Thermal (b) Mechanical

Fig. 3: Prior knowledge on system dynamics imposed in the developed approach. For thermal system it is assumed that poles, which are used in the orthonormal basis functions, lie on the real axis since the thermal dynamics are first order, and for mechanical systems often a frequency region and damping ratio of resonance modes is known.

method by applying a window function, which is true for 1st order thermal dynamics, and can be locally approximated in a window $[k-n:k:k+n]$ around the k-th DFT bin. Then both terms are approximated as

$$\begin{aligned} G(e^{i\omega_{k+r}}) &= \sum_{b=1}^{N_b} \theta_{G_b} B_b(e^{i\omega_{k+r}}) \\ T(e^{i\omega_{k+r}}) &= \sum_{b=1}^{N_b} \theta_{T_b} B_b(e^{i\omega_{k+r}}) \end{aligned} \tag{8}$$

where $G(e^{i\omega_{k+r}})$ and $T(e^{i\omega_{k+r}})$ are linearly parameterized by a set of basis functions $B_b(e^{i\omega_{k+r}})$ and their parameters $\theta_{G_b}, \theta_{T_b}$.

The basis functions $B_b(e^{i\omega_{k+r}})$ used in (8) are constructed as Orthonormal Basis Functions (OBF). The Discrete time OBFs are generated by a series connection of all-pass elements. A general form [24] is given by

$$B_b(z) = \left(\frac{z\sqrt{1-|\zeta_n|^2}}{z-\zeta_n}\right)\prod_{k=0}^{n-1}\left(\frac{1-\bar{\zeta_k}z}{z-\zeta_k}\right) \tag{9}$$

where $\zeta = \{\zeta_0, \zeta_1, \ldots, \zeta_p\}$ are the pre-specified poles p for the all pass functions. The parameterization in (9) is known as the Takenaka-Malmquist [25], [24] functions and are used in (8) to approximate the local function as a linear combination of rational functions.

The local approximation in (8) can be improved by imposing prior knowledge on the system dynamics. Imposing prior knowledge on the local approximation in (8) is straightforwardly done by selecting the locations of the poles, shown in the complex plane in Fig. 3, of the basis functions B_b. Clearly, if the basis functions B_b span the true model class of $G(e^{i\omega_k})$ and $T(e^{i\omega_k})$ then (8) can approximate the FRF in the considered window arbitrarily well. For thermal systems [20]

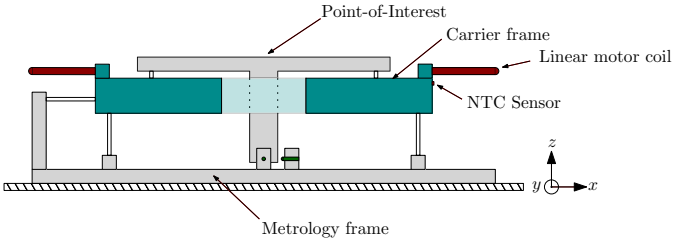

Fig. 4: 2D cross section of the PSA, indicating the carrier frame, metrology frame, linear motor coil and sensor location.

the poles lie on the real axis, and for mechanical system [3], often a frequency region or damping ratio is known.

By then using an appropriate excitation signal, e.g., a random phase multisine, a local estimate of the transient component $T(e^{i\omega_k})$ is constructed for a specific DFT bin k. This transient estimation is then used to correct the estimated $G(e^{i\omega_k})$. This process is repeated by performing a local parametric estimation procedure at each DFT bin to construct the final non-parametric FRF. The proposed method is a generalization of previous methods [26], and simplifies to the well known Local Polynomial Method [15] by selecting $\zeta = 0$.

III. Thermal response in a mechatronic system

The following section presents a detailed exposition of the experimental setup, shown in Fig. 1, including its excitation and data-acquisition system.

A. Thermal actuator

An 2D-schematic overview of the setup is shown in Fig. 4 that shows the relevant components and sensor location. For a mechanical analysis, the linear motor would be used to induce force on the carrier frame. For the thermal response, a different approach is required. Since the setup is stationary, the linear motor stator is removed and its rotor, the coils, are maintained. To inject power into the carrier frame, a current is induced into the motor coils that generates heat that propagates through the motor mounts into the carrier frame. To maintain a specific power input, the current and voltage are measured and the power amplifier is put in feedback, as shown in Fig. 5, such that a reference power input is tracked. This allows the consideration of the full thermal system G_T in open loop, while the power control is kept in closed loop.

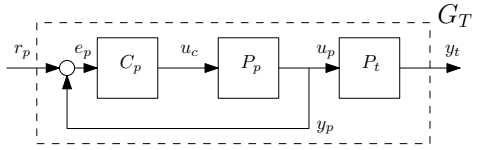

Fig. 5: The control diagram for the experimental setup. The power amplifier P_p is placed in feedback using controller C_p. The identification considers the transfer between r_p and y_t, i.e., the system P_t is considered as open loop, and together with the closed-loop current control forms the full system G_T.

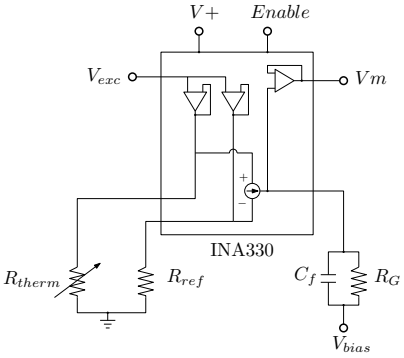

Fig. 6: Electrical diagram of the INA330 that provides an excitation current to the NTC sensor R_{therm} and reference resistor R_{ref}. The current difference is amplified and is provided as a measurement output V_m.

B. Thermal measurements

Position measurements are readily performed using laser interferometry or capacitive probes, however, temperature measurements remain challenging. Non-contact measurements of temperature are possible using long-wave infrared cameras, but these are often limited in accuracy and resolution. For the experimental setup considered in this work use is made of contact measurements using thermistors, which are resistors with a Negative Temperature Coefficient (NTC), i.e., their electrical resistance changes with temperature.

These NTCs are accurate and inexpensive, however, are prone to self-heating due to the Joule heating of the resistor. Use is made of an operational amplifier, the INA330 shown in Fig. 6, that provides the excitation current to the thermistor R_{therm} and reference resistor R_{ref} that are then compared and amplified to a voltage using R_g which provides the measurement output V_m. By careful selection of the components, a temperature resolution within the mK range is achieved.

C. System identification

The following section present system identification measurements on the PSA, comparing the two approaches presented in Sec. II. It shows that significant improvement in estimation quality, and a reduction in measurement time, can be achieved using the proposed local methods compared to classical spectral methods.

1) Setup: The identification setting is shown in Fig. 5, i.e., the open-loop G_T plant is identified using an excitation power r_p [W] input and temperature measurement y_t [K] output. The excitation r_p a random phase multisine [15] limited to 0.1 [Hz], with a peak value of 5 [W] centered around an offset of 5 [W]. Measurements using a 16-bit dspace system at 1000 [Hz] are down sampled to $F_s = 1$ [Hz] to facilitate post processing The multisine has a period length of $L = 1$ [h], that is repeated $P = 48$ times, yielding a total dataset of $F_s LP = 172800$ samples. During the measurements, the stage is fixed in 6 DOF to the base plate, however, deformations can still cause the structure to deform thus shifting the POI. The prescribed

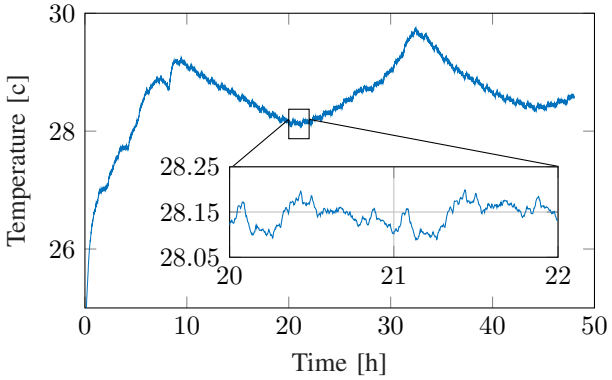

Fig. 7: Temperature response of the experimental setup over a 48 hour period. A zoomed section of period $[20-22]$ shows two periods of the periodic response, that is small when compared to the overall transient response of the system. This shows that there is a large environmental disturbance, causing a strong transient response.

poles as described in Sec. II-B are spread uniformly on the real axis at low frequencies since the true system poles of the experimental setup are unknown.

2) Transient response: Although multiple temperature sensors are present on the setup, to facilitate presentation a single channel is used as shown in Fig. 4. The output dataset is presented in Fig. 7, it shows the temperature over a 48 hour period. It is seen that the output has an initial 1st order step response, due to the offset in the excitation signal, followed by a higher order response to the full spectrum multisine. The additional zoom-plot provides a detailed view of 2 periods, it clearly shows that the small and relatively fast steady state dynamic response is superimposed onto a much larger and slower transient response caused by initial excitation and the $24-$hour cycle of the environment.

3) Full dataset: Estimating the FRF using the full dataset as shown in Fig. 7, i.e., $P = 48, T = 0$ where T denotes the amount of periods that are removed from the estimation, results in an FRF as shown in Fig. 8a. A comparison is made between the traditional method using two different window functions, and the proposed approach (LRMP). Moreover, by using the method shown in Sec. II-B an explicit estimate of the transient component $T(e^{i\omega_{k+r}})$ is shown. The results show that the spectral estimate is dominated by the transient component, resulting in a poor estimate with high variance. The LRMP method estimates and removes the transient $T(e^{i\omega_{k+r}})$ from the plant estimation $G(e^{i\omega_{k+r}})$ resulting in a good estimate with low variance. It must be noted that the true system G_0 is unknown, i.e., the results are judged on the obtained variance and expected dynamical behavior.

4) Reduced dataset: The previous result in Fig. 8a showed that using a long dataset, an accurate estimate of the FRF can be achieved. This is often not possible, due to limited measurement time or the availability of a suitable dataset. The temperature response in Fig. 7 reveals that during periods

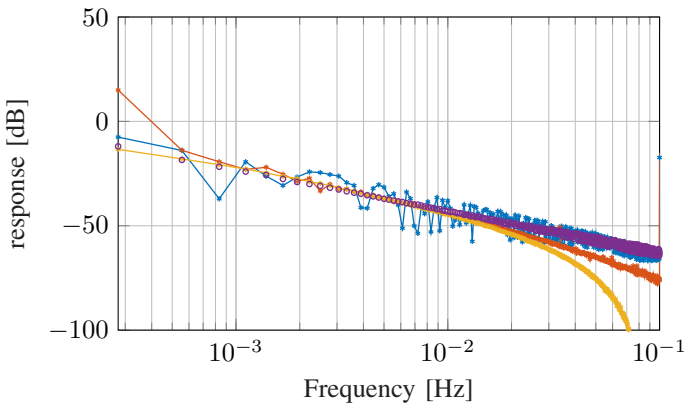

(a) $P = 48, T = 0$

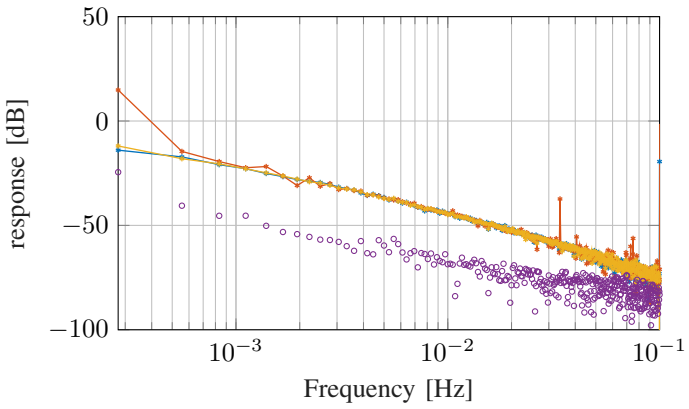

(b) $P = 2, T = 20$

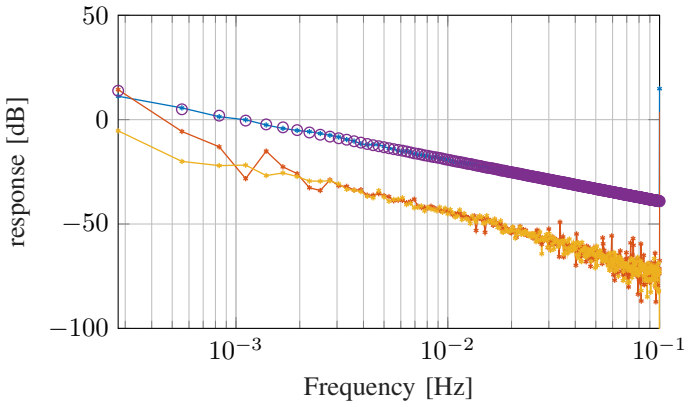

(c) $P = 2, T = 0$

Fig. 8: A comparison is shown between the traditional approach using the spectral method method with a boxcar (—*—) and Hanning (—*—) window, and the proposed approach LRMP (—*—) and the estimated transient (◦). The subfigures indicate the results of applying the proposed approach on different data sections of the full dataset shown in Fig. 7. Here, P denotes the amount of periods used, and T denotes the amount of initial periods removed.

$20, 21$ both the excitation and environmental transients are small. A reduced dataset consisting of only this subset of periods is used for FRF estimation, i.e., $P = 2, T = 20$, and the results are shown in Fig. 8b. It shows that the estimated transient is relatively small, and that both the traditional and proposed method provide a good estimate of the FRF with low variance. It shows that using the Hanning window introduces a bias, as shown in the first few frequency points, caused by the convolution with the window function [15] and the non-zero DC component of the DFT. Using the interval $P = [20, 21]$ provided a good FRF estimate, however, this requires that both the excitation and environmental transients are small. This often requires long measurements during a specific time of the day, which is not always feasible for industrial applications. Therefore, using $P = 2, T = 0$, i.e., using the first 2 periods, results in an FRF estimate as shown in Fig. 8c. It shows that the spectral method using the boxcar window is completely dominated by the transient response, and using the Hanning window results in an estimation bias. Here, the LRMP provides fast and accurate FRF estimation, similar to the ideal case when using $P = 2, T = 20$, even under strong transient conditions.

IV. Conclusion

In this paper the challenges in thermo-mechanical behavior in precision motion control are outlined, and a new approach to system identification is provided. The proposed approach is capable of estimating and removing transient components during the FRF estimation. The proposed method is applied to a relevant thermo-mechanical precision stage application setup, where it is shown that the method achieves superior estimation quality, a reduced variance and shorter measurement times when compared to traditional spectral analysis based approaches.

Acknowledgment

This work is supported by the Advanced Thermal Control consortium, which is gratefully acknowledged for providing the means to realize the experimental setup, and is part of the research programme VIDI with project number 15698, which is (partly) financed by the Netherlands Organization for Scientific Research (NWO).

References

[1] H. Butler, "Position control in lithographic equipment [applications of control]," *IEEE Control Systems*, vol. 31, no. 5, pp. 28–47, 2011.

[2] A. N. Taru, P. Nuij, and M. Steinbuch, "Model-Based Drift Control for Electron Microscopes," *IFAC Proceedings Volumes*, vol. 44, no. 1, pp. 8583–8588, Jan. 2011.

[3] T. Oomen, "Advanced Motion Control for Precision Mechatronics: Control, Identification, and Learning of Complex Systems," *IEEJ Journal of Industry Applications*, vol. 7, no. 2, pp. 127–140, 2018.

[4] E. Evers, M. van de Wal, and T. Oomen, "Synchronizing Decentralized Control Loops for Overall Performance Enhancement: A Youla Framework Applied to a Wafer Scanner," in *IFAC World Congress*, Jul. 2017.

[5] J. van Zundert and T. Oomen, "Inverting Nonminimum-Phase Systems from the Perspectives of Feedforward and ILC," in *IFAC World Congress 2017*, Toulouse, France, Jul. 2017.

[6] A. J. Fleming and K. K. Leang, *Design, Modeling and Control of Nanopositioning Systems*, ser. Advances in Industrial Control. Cham: Springer International Publishing, 2014.

[7] W. Ohnishi, T. Beauduin, and H. Fujimoto, "Preactuated multirate feedforward for a high-precision stage with continuous time unstable zeros," *IFAC-PapersOnLine*, vol. 50, no. 1, pp. 10 907–10 912, Jul. 2017.

[8] L. Blanken, G. Isil, S. Koekebakker, and T. Oomen, "Data-Driven Feedforward Learning using Non-Causal Rational Basis Functions: Application to an Industrial Flatbed Printer," in *2018 American Control Conference (ACC 2018)*. Wisconsin, United States: Institute of Electrical and Electronics Engineers (IEEE), Jun. 2018.

[9] J. Guo, "Positioning Performance Enhancement via Identication and Control of Thermal Dynamics: A MIMO Wafer Table Case Study," Master's thesis, Eindhoven University of Technology, May 2014, cST 2014.070.

[10] T. Oomen, E. Grassens, and F. Hendriks, "Inferential Motion Control: Identification and Robust Control Framework for Positioning an Unmeasurable Point of Interest," *IEEE Transactions on Control Systems Technology*, vol. 23, no. 4, pp. 1602–1610, Jul. 2015.

[11] S. Skogestad and I. Postlethwaite, *Multivariable feedback control: analysis and design*, 2nd ed. Chichester: Wiley, 2009.

[12] A. H. Koevoets, J. van der Sanden, and T. Ruijl, "Thermal-elastic compensation models for position control," in *Proceedings of the ASPE Annual Meeting*, vol. 2009, 2009.

[13] T. Oomen, R. van Herpen, S. Quist, M. van de Wal, O. Bosgra, and M. Steinbuch, "Connecting System Identification and Robust Control for Next-Generation Motion Control of a Wafer Stage," *IEEE Transactions on Control Systems Technology*, vol. 22, no. 1, pp. 102–118, Jan. 2014.

[14] T. Oomen and O. Bosgra, "System identification for achieving robust performance," *Automatica*, vol. 48, no. 9, pp. 1975–1987, Sep. 2012.

[15] R. Pintelon and J. Schoukens, *System identification: a frequency domain approach*, 2nd ed. Hoboken, N.J: John Wiley & Sons Inc, 2012.

[16] A. Karimi and Y. Zhu, "Robust H-infinity Controller Design Using Frequency-Domain Data," ser. 19th IFAC World Congress, Cape Town, South Africa, 2014.

[17] R. Voorhoeve, R. de Rozario, and T. Oomen, "Identification for motion control: Incorporating constraints and numerical considerations," in *American Control Conference (ACC), 2016*. IEEE, 2016, pp. 6209–6214.

[18] E. Geerardyn, M. L. D. Lumori, and J. Lataire, "FRF Smoothing to Improve Initial Estimates for Transfer Function Identification," *IEEE Transactions on Instrumentation and Measurement*, vol. 64, no. 10, pp. 2838–2847, Oct. 2015.

[19] R. Voorhoeve, A. van Rietschoten, E. Geerardyn, and T. Oomen, "Identification of high-tech motion systems: An active vibration isolation benchmark," *IFAC-PapersOnLine*, vol. 48, no. 28, pp. 1250–1255, 2015.

[20] G. Monteyne, G. Vandersteen, R. Pintelon, and D. Ugryumova, "Transient suppression in FRF measurement: Comparison and analysis of four state-of-the-art methods," *Measurement*, vol. 46, no. 7, pp. 2210–2222, Aug. 2013.

[21] R. Relan, K. Tiels, J.-M. Timmermans, and J. Schoukens, "Estimation of Best Linear Approximation from Varying Operating Conditions for the Identification of a Li-ion Battery Model," *IFAC-PapersOnLine*, vol. 50, no. 1, pp. 4739–4744, 2017.

[22] T. van Keulen, L. Huijben, and T. Oomen, "Identification of Control-Relevant Diesel Engine Models Using a Local Linear Parametric Approach," *IFAC-PapersOnLine*, vol. 50, no. 1, pp. 7836–7841, Jul. 2017.

[23] E. Evers, B. d. Jager, and T. Oomen, "Improved Local Rational Method by incorporating system knowledge: with application to mechanical and thermal dynamical systems," in *18th IFAC Symposium on System Identification (SYSID 2018)*, Stockholm, Sweden, Jul. 2018.

[24] B. Ninness and F. Gustafsson, "A unifying construction of orthonormal bases for system identification," *IEEE Transactions on Automatic Control*, vol. 42, no. 4, pp. 515–521, 1997.

[25] S. Takenaka, "On the Orthogonal Functions and a New Formula of Interpolation," *Japanese journal of mathematics: transactions and abstracts*, vol. 2, no. 0, pp. 129–145, 1925.

[26] R. Voorhoeve, A. van der Maas, and T. Oomen, "Non-parametric identification of multivariable systems: A local rational modeling approach with application to a vibration isolation benchmark," *Mechanical Systems and Signal Processing*, vol. 105, pp. 129–152, May 2018.